LA-UR -92-572

CONF-

LA-UR--92-572

DE93 008700

Los Alamos National Laboratory is operated by the University of California for the United States Department of Energy under contract W-7405-ENG-36

TITLE: PROTEIN RESPONSE TO LIGATION REACTIONS IN MYOGLOBIN

AUTHOR(S): R. Brian Dyer, CLS-4
Timothy P. Causgrove, CLS-4

SUBMITTED TO: Proceedings of SPIE International Society of Optical Engineering (Biomolecular Spectroscopy III)

DISCLAIMER

Los Alamos National Laboratory
Los Alamos, New Mexico 87545

FORM NO. 836 R4
ST. NO. 2629 5/91

Protein Response to Ligation Reactions in Myoglobin

Timothy P. Causgrove and R. Brian Dyer*

Photochemistry and Photophysics Group (CLS-4, Mail Stop J567)
University of California, Los Alamos National Laboratory, Los Alamos, NM 87545

ABSTRACT

The protein response to the photodissociation, escape and subsequent rebinding of carbon monoxide in myoglobin is studied using time-resolved infrared (TRIR) spectroscopy. All phases of these reactions are investigated, from ultrafast phenomena (picoseconds) to relatively slow processes (milliseconds). Conformational changes in myoglobin (Mb) are detected by time-resolved infrared absorption changes in the amide I band. On the hundreds of nanoseconds to milliseconds timescale, a 'real-time' apparatus is used. This apparatus is based on a tunable diode laser operating in the region of 1650 cm^{-1}. The time course of changes in the amide I band are shown to follow the recombination of CO with photolyzed Mb. On the basis of the rise times of the amide I and Fe-CO signals, it is concluded that protein motion is complete within 100 ns. A time-resolved difference spectrum in the amide I region is generated from single wavelength transients taken throughout the amide I envelope. A static difference spectrum is also generated by subtracting FTIR spectra of carbonmonoxy and deoxy myoglobin. The two difference spectra are compared and are interpreted in terms of the three-dimensional structures of deoxy and carbonmonoxy Mb. Preliminary picosecond TRIR data are also given for the ultrafast response of the protein immediately following photodissociation of CO.

1. INTRODUCTION

The structure and dynamics of conformational changes in hemoglobin resulting in cooperativity in ligand binding has been a long-standing problem in biophysics. The use of myoglobin (Mb) as a simpler, non-cooperative model protein has been established through spectroscopic and crystallographic examination. A central question in Mb ligand binding is the dynamics and energetics of motion of the protein relative to the heme. This problem has been illustrated by examining the carefully characterized X-ray crystal structure of Mb. If this compact structure remained fixed in solution, no pathway would exist for small ligands such as CO and O_2 to diffuse from solution into the heme binding site.[1] Clearly, fluctuations of the protein in solution must play an important role in the function of the enzyme. Time-resolved infrared (TRIR) spectroscopy is uniquely suited as a probe for these processes, particularly the behavior of the protein, which generally is not observable by other spectroscopies.[2] TRIR spectroscopy also has the capacity to study protein motions with minimal interference from the heme, in contrast to techniques based on visible light such as resonance Raman and circular dichroism.

The use of time-resolved difference spectra in the amide I region provides a powerful tool for the study of protein dynamics. It has long been known that infrared spectra in the amide region are sensitive to protein secondary conformation.[3] Recent advances in equipment and techniques, including difference spectroscopy and various resolution enhancement techniques, have permitted researchers to quantitatively predict secondary structures from infrared spectra,[4,5,6,7,8] particularly in the amide I region.[5,6] In light of these results, it is now possible to study secondary structures in time-resolved experiments on protein dynamics and function

The ligation reactions of small molecules such as CO with the heme site of Mb exemplify the mechanisms available to O_2, potentially revealing the molecular details of the enzyme function. CO is an ideal candidate for initial time-resolved IR experiments in the amide I region because it is easily photolyzed and the structure of both MbCO and unligated Mb have been extensively studied by crystallographic methods.[9,10] In addition, CO ligation is often preferred in time-resolved spectroscopic studies due to the stability of MbCO in solution and because CO exhibits little geminate recombination.[11,12] Photolysis of CO from Mb and its recombination processes have been studied by a

large array of techniques, including UV-Vis absorption;[11,13] molecular dynamics,[14] time-resolved CD,[15] TRIR,[16,17,18,19] time-resolved resonance Raman,[20] and photoacoustic calorimetry.[21,22] Of these techniques, TRIR holds the most promise for providing detailed information on dynamics of the protein itself.

Infrared spectroscopy has already played a large role in investigating the ligand binding dynamics in Mb and Hb from the subpicosecond[17,18] to millisecond[16,19] time scale. These studies probed the Fe-CO bleach at 1943 cm^{-1} and in some cases, the 2135 cm^{-1} absorption of photolyzed CO trapped in the heme pocket. Dynamics of the protein, however, have yet to be probed by TRIR spectroscopy of the protein vibrations themselves. Here we report results on the motions of the protein in response to ligation reactions, monitored in the amide I region centered about 1650 cm^{-1}.

2. MATERIALS AND METHODS

Carbonmonoxy myoglobin (MbCO) was prepared by dissolving lyophilized sperm whale myoglobin (Sigma M-0380) or horse skeletal muscle myoglobin (Sigma M-0630) in 50 mM phosphate buffer, pD 7.4 (in D_2O). The heme was reduced with 5 mM sodium dithionite and liganded with CO by several cycles of degassing and back-filling with CO. Final samples were 0.8-2.0 mM MbCO held in 50 μm sealed cells with CaF_2 windows. Samples used in the picosecond experiments were more concentrated (4.6 mM) and pathlengths were either 50 or 100 μm. FTIR spectra of the samples were taken on a Mattson Galaxy Series FTIR 5000.

Real-time TRIR measurements (10^{-8} to 10^{-1} s) were obtained using an apparatus that has been described previously[2] with the following minor modifications. The InSb detector was replaced with a HgCdTe detector and biased amplifier (risetime ~300 ns). The laser diode used as a probe source was temperature tunable between 1605 and 1725 cm^{-1} with a mode spacing of about 4.5 cm^{-1}. Each mode was tunable by about 1 cm^{-1}, leaving small gaps inaccessible to the probe source. The laser pump pulse was supplied by the 532 nm second harmonic of a Nd:YAG laser, with typical pulse energies of about 120 μJ. The measured decay was generated by subtracting traces taken with the Nd:YAG laser blocked from those with the laser unblocked.

Ultrafast TRIR measurements were obtained by means of a pump-probe experiment, shown schematically in Figure 1, in which the time resolution is accomplished by optical delay.[23] The visible pump (photodissociation) pulse (1.7 ps, 595 nm, 3-10 μJ) is generated by a dye laser synchronously pumped by a frequency doubled, mode-locked Nd:YAG laser (Coherent Antares 76) then amplified in a three stage dye amplifier pumped at 30 Hz and 532 nm by a Nd:YAG regenerative amplifier (Quantel RGA60). The infrared probe pulse is generated in a two step nonlinear mixing process. In the first step, the difference frequency between the 1064 nm pulses from the regenerative amplifier and the amplified dye pulse is generated in a potassium titanyl phosphate (KTP) crystal cut at 65° for type II phase matching. This generates a near infrared pulse at 1.3 μm. The mid-infrared probe pulse is generated in a second step by differencing the residual 1064 nm light with the 1.3 μm light in a silver thiogallate ($AgGaS_2$) crystal cut at 46° for type II difference frequency mixing. Tuning the dye laser yields infrared pulses (1.7 ps, 100 nJ) tunable from 1200 to 2500 cm^{-1}. The infrared light is split into "sample" and "reference" pulses. The time of arrival of the pump pulse is adjusted using a computer controlled optical delay line (Klinger). It is then made colinear with the infrared "sample" pulse using a dichroic mirror and both are focused to a 100 μm spot on the sample. The infrared "sample" and "reference" intensities are then detected with matched HgCdTe detectors and a dual channel boxcar integrator and ratioed to correct for shot-to-shot amplitude fluctuations. The adverse effects of long term laser drift are minimized by synchronously chopping the pump at half the repetition rate (15 Hz) to yield alternating "light" and "dark" signals from which ΔA is determined at each optical delay. Before and after each protein measurement, the zero-of-time and the instrument temporal response (dependent solely on the pump/probe cross-correlation width) are determined by substituting for the sample a Si wafer in which the pump causes an instantaneous decrease in transmission of the probe.[24] The temporal response varies with laser conditions but generally is well described by a $sech^2$ function of FWHM = 3.5 ps.

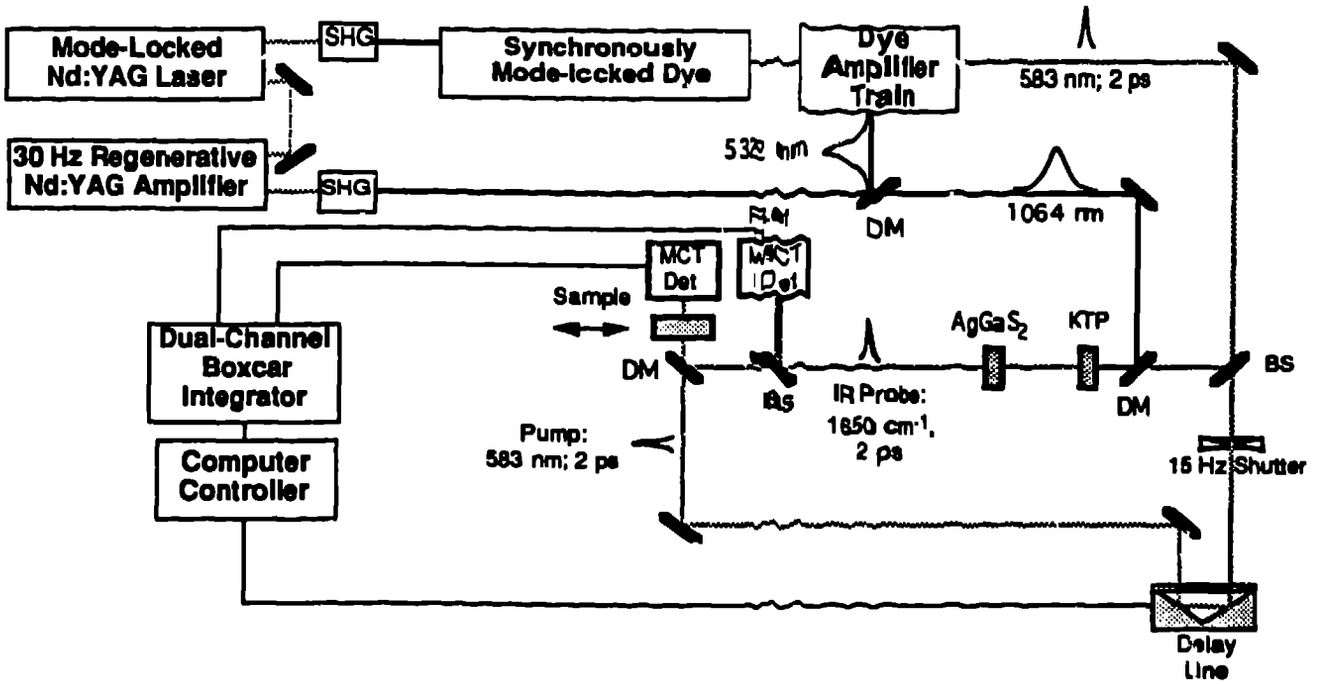

Figure 1: Picosecond time-resolved infrared spectroscopy apparatus.

3. RESULTS

3.1 Myoglobin dynamics from 100 ns to 10 ms.

Typical decay traces of infrared absorption changes at 1943 and 1660 cm^{-1}, following laser photodissociation of CO, are shown in Figure 2. The traces were taken under identical conditions (i.e., using the same amplifier and HgCdTe detector) and were normalized to the same peak amplitude. Although the signal at 1660 cm^{-1} is smaller, the signal-to-noise ratios are similar due to greater laser power from the lower frequency diode as well as higher responsivity of the detector. Analysis of the traces was done using the so-called A+B second order kinetics, fitting the data to the equation

$$\Delta A = \varepsilon l[Mb](1-[Mb]/[CO])/\{\exp(kt([Mb]-[CO]))-[Mb]/[CO]\} + b$$

where [Mb] is the concentration of unliganded Mb immediately after the flash, [CO] is the initial concentration of free CO, and k is the second-order rate constant. The initial concentration of CO was taken as [Mb] + 0.8 mM, the concentration of saturated CO solution. The second-order rate constant was a variable in the fitting, and the extinction coefficient, ε, was fixed at 1920 $M^{-1}cm^{-1}$ as determined by Dixon, et al.[16] The path length, l, was fixed at 50 μm. The additional parameter *b* was required due to a small baseline offset. This offset is a small fraction of the total signal and is probably due to thermal effects since both its magnitude and sign are independent of probe wavelength. The resulting fits gave second-order rate constants of 3.8 (1943 cm^{-1}) and 4.1 (1660 cm^{-1}) x 10^5 $M^{-1}s^{-1}$, within experimental error of each other, but slightly lower than the value of 5.0 x 10^5 $M^{-1}s^{-1}$ determined by UV-Vis spectroscopy (Gibson et al. 1986). The best fit at 1943 cm^{-1} was obtained with an initial concentration of unliganded myoglobin of 0.46 mM, corresponding to ~60% photolysis. For fitting of data acquired at 1660 cm^{-1}, [Mb] was fixed at 0.46 mM and the extinction coefficient determined by fitting was 367 M^{-1} cm^{-1}. Errors may be introduced in this analysis by the assumption of a saturated CO solution or by slightly different photolysis efficiencies between the two measurements.

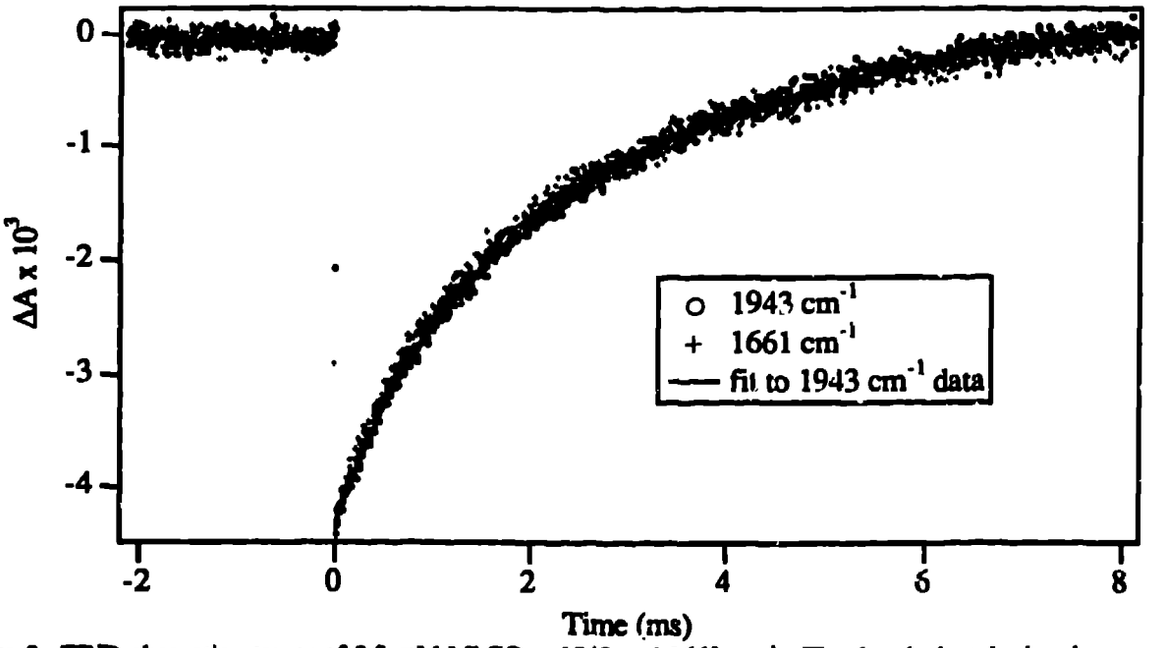

Figure 2. TRIR absorption traces of 0.8 mM MbCO at 1943 and 1660 cm^{-1}. The data had peak absorbance changes of 4.3×10^{-3} and 1.6×10^{-3}, respectively. Each of the decay traces is an average of data from 1600 individual laser shots. The solid line is a three-parameter fit to the 1943 cm^{-1} data according to A+B second-order kinetics.

Transients were also taken at several wavelengths using faster amplifiers in an attempt to resolve kinetics due to the motion of the protein in response to CO photodissociation. The rise of the transient at 1660 cm^{-1} is compared in Figure 3 to the Fe-CO bleach at 1943 cm^{-1}, which is instantaneous on this timescale since the Fe-CO bond is broken within 300 fs.[18] Clearly the risetimes of these two transients are indistinguishable and therefore both instrument limited.

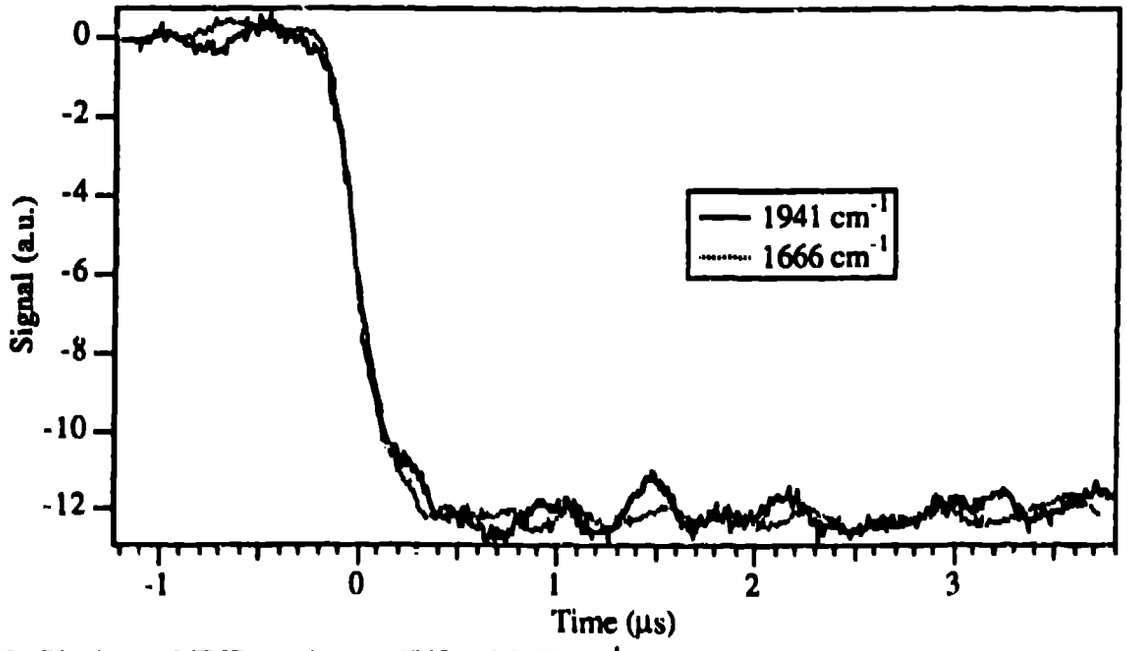

Figure 3. Risetimes of TRIR transients at 1943 and 1660 cm^{-1}.

For all wavelengths probed in the amide I region, the rise of the transient absorption was limited by the response of the system, all showing a 10-90% rise time of 300 ns; with deconvolution, changes on a time scale down to about 100 ns would be observable with the present system. We conclude that protein motion, or at least the portion observable in the amide I IR band, is complete within 100 ns.

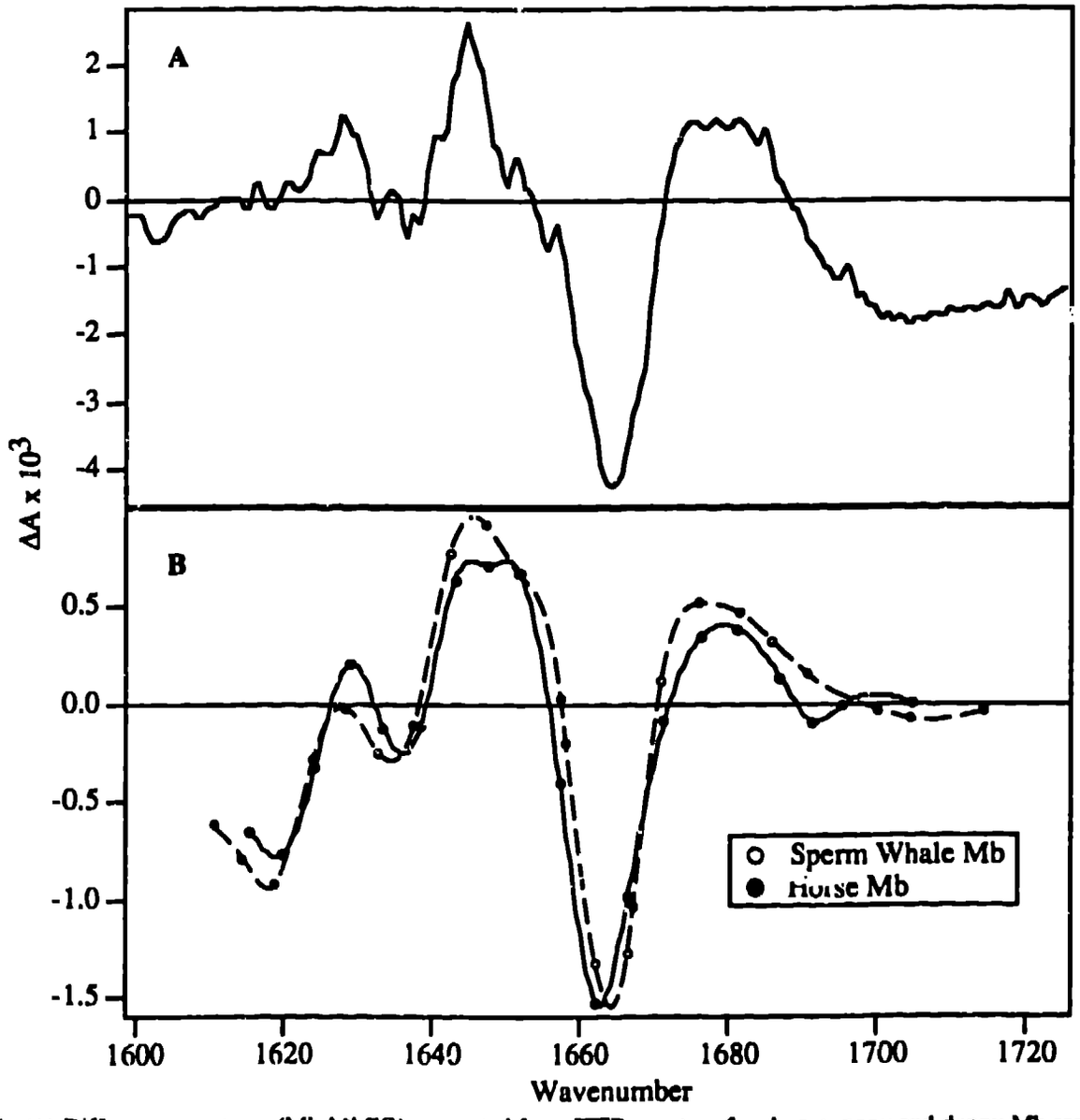

Figure 4. (A) Difference spectrum (Mb-MbCO) generated from FTIR spectra of carbonmonoxy and deoxy Mb samples of 2 mM sperm whale Mb. (B) Difference spectra generated from initial amplitudes of IR transients of 0.8 mM sperm whale Mb (o) and horse skeletal muscle Mb (•) in the amide I region. The symbols are the actual data; the lines are cubic spline interpolations.

By tuning the frequency of the probe source, transients such as those shown in Figure 3 were generated across the amide I band from 1608 cm^{-1} to 1723 cm^{-1}. The initial amplitude of each of these transients was recorded and plotted against frequency to create a Mb-MbCO difference spectrum (Figure 4B). The spectrum contains several features, the most prominent of which is peaked at 1664 cm^{-1} with an absorbance change of 1.5×10^{-3} (using 1.6 mM MbCO), compared to an absorbance of 0.8 for the

total amide I peak. The spectrum shows several other features, all of which are reproducible. The width of most peaks in the difference spectrum appears to be about 8-10 cm^{-1}. The TRIR difference spectrum was also examined for horse skeletal muscle Mb, which has a slightly different amino acid sequence than sperm whale Mb. The largest difference between the two samples is in the high frequency region, where horse Mb shows a sharper 1680 cm^{-1} peak than sperm whale myoglobin with no signals observable in the 1700-1720 cm^{-1} range. Figure 4A shows the static difference spectrum (Mb-MbCO) obtained by subtracting FTIR spectra of carbonmonoxy and deoxy Mb for sperm whale Mb. While the baseline is clearly not flat in this region, all of the major features in the TRIR spectrum are reproduced in the static FTIR spectrum. This is convincing evidence that the spectrum obtained for MbCO 100 ns after photodissociation of CO is essentially identical in the amide I region as the static spectrum of deoxy Mb.

3.2 Ultrafast Myoglobin dynamics.

We have directly observed the photodissociation of CO from the heme binding site in a picosecond TRIR experiment. The time-resolved bleaching of the Fe-CO absorption at 1943 cm^{-1} is indistinguishable from the instantaneous instrument response, determined before and after the protein measurement using a Si wafer. This observation is consistent with femtosecond UV-Vis[13] and TRIR[18] measurements which indicate that CO photodissociation occurs in less than 150 fs, probably on the timescale of one vibrational period of the Fe-CO stretch (520 cm^{-1}, 64 fs). The Fe-CO infrared transient was recorded for 100 ps following the pump pulse with no observable decrease in the bleach which could be attributed to geminate recombination, indicating that the barrier to recombination must form rapidly. The absence of rapid geminate recombination of CO is typical for heme proteins and has been attributed to electronic (spin) barriers[13] and frictional forces due to iron displacement opposing rebinding.[25]

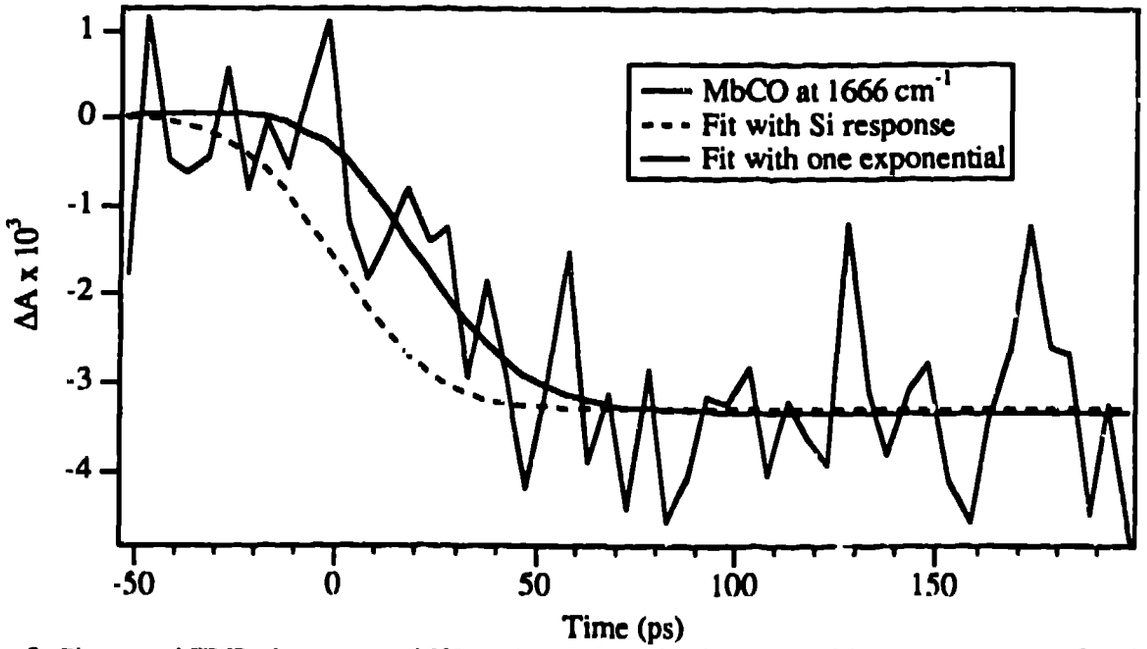

Figure 5. Picosecond TRIR absorption at 1666 cm-1, together with the measured instrument response function (dashed line) and the best fit to the data of a convolution of this function with an exponential function (τ = 15 ps).

The protein response immediately following the photodissociation of CO was probed in additional picosecond TRIR experiments. The infrared transient monitored at 1666 cm^{-1}, the peak of the largest amide I difference band in the μs spectrum, is shown in snown in Figure 5. The intensity of this signal

is about one third that of the CO bleach at 1943 cm^{-1}, exactly what is expected based on the nanosecond difference spectrum. The experimentally determined instrument (Si) response, which is best fit with a $sech^2$ function of FWHM = 20 ps, is also shown. The best fit to the transient, the convolution of the 20 ps $sech^2$ instrument response function with a 15 ps exponential function, is also plotted in Figure 5. Positive transients (absorptions) were also observed at 1645 and 1680 cm^{-1}, although the signal-to-noise at these probe wavelengths was insufficient to permit fitting the data to extract dynamics.

4. DISCUSSION

One of the main complications in TRIR spectroscopy is artifacts from thermal changes in the sample due to heating by the pump pulse. In our experience, these artifacts normally appear as a bleach and have a lifetime of several milliseconds, longer than the heme-CO recombination in myoglobin. The observation in Figure 2 that the kinetics of the heme-CO bleach and the amide I changes are the same indicates that the signals are free from thermal artifacts. This is also evident from Figure 4 in that the change in absorption tends to zero at the high frequency end of the spectrum. Figure 3 also indicates that any changes in protein conformation are slower than the time scale of the measurement; if the kinetics were limited by protein motion, the decay of the 1660 cm^{-1} trace would be slower than the CO recombination.

The assignment of infrared band shapes and subbands from steady-state FTIR spectra to specific secondary structures is currently an active area in the literature. The main techniques for resolving subbands in the amide I region have been resolution enhancement by Fourier self-deconvolution[8,26] and generation of second derivative spectra.[4,6] It should be noted that both of these techniques require very high signal-to-noise and careful elimination of water vapor bands. Recently criteria for the subtraction of water and water vapor backgrounds have allowed consistent bands beneath the amide I envelope to be assigned to specific secondary structures.

There are many complications in the comparison of these assignments to the features seen in the Mb difference spectra shown in Figure 4. First, the difference spectrum is the sum of all changes in the protein, which may involve a complex superposition of bands. Also, there may be contributions to the difference spectra from amino acid side chain vibrations. These are generally considered small when measuring the overall amide I spectrum; however, the difference spectrum is sensitive to only those vibrations that change, which may increase the relative contribution of specific side chain vibrations that undergo large conformational changes. Comparison of the area of the overall amide I peak to that of the 1664 cm^{-1} bleach in Figure 4 (corrected for photolysis efficiency) gives a ratio of 350:1, corresponding to a bleach of less than one backbone CO vibration. Therefore, the contribution of side chain vibrations in the difference spectrum must be considered. The role of Arg45 (CD3) in particular has been the subject of several examinations.[9,22,27] X-ray structures have shown that Arg45 forms a salt bridge with one of the propionate groups of the heme and that the breaking of the salt bridge is an important (and one of the largest) structural differences between the CO and deoxy forms of Mb.[9] This may be important in the interpretation of the IR difference spectra as arginine is one of the amino acids likely to show side chain vibrations in the 1600-1700 cm^{-1} region. Horse Mb does not have arginine; this may be reflected in the high frequency end of the horse TRIR difference spectrum, which is very different from sperm whale Mb (Figure 4B).

Tables of amide I band assignments have been made by Dong, et al.[4] for proteins in H_2O solution and by Susi and Byler[8] for a standard protein set in D_2O. Although there is general agreement between the two assignments, there are some differences in the exact frequency assignments. The most straightforward assignment is that for α–helix, which shows only a single narrow band at 1653-1656 cm^{-1}. Mb, which is 80% α–helix, is dominated by a single peak at 1654 cm^{-1}.[4] Interestingly, the Mb difference spectra have an isosbestic point near this frequency, consistent with the finding that the helix structures of Mb are quite similar between the CO and deoxy forms, but only shift relative to each other.[9] The bleach at 1664 cm^{-1} in Figure 4 is in the region assigned to turn structures; bands at 1676 cm^{-1} (a transient absorption in Figure 4) have been assigned to either turn or extended chain conformations. The other main absorption at 1645 cm^{-1} is in the area assigned to unordered structure. Bands at lower

frequency have been assigned to both either β-sheet[4] or general β-type[8] structures. In the case of Mb, the lower frequency signals must represent bleaching of the small regions of β-turns since the protein contains no β-sheet.[9,10] In order to make specific assignments to each of the spectral features in Figure 4, additional data is required. Further information on the interpretation of these spectra could be gained from perturbed systems. For example, the contribution of some ionizable side chains is in principle available from pH-dependent studies; other side chain vibrations can be addressed through selective isotopic labeling and site-directed mutagenesis.

The most important result of this study is the measurement of the protein dynamics associated with the photodissociation of CO from the heme. What is clear from the previous discussion is that the dynamics measured are associated with the changes in protein backbone conformation to which the amide I vibrations are most sensitive, and possibly the motion of specific side chains which also have absorptions in this spectral region. The 'real-time' TRIR measurements indicate that the conformational change from the carbonmonoxy to the deoxy form is over within 100 ns of the photodissociation.

The picosecond TRIR experiments give information on the initial stages of protein motion, and provide a connection between molecular dynamics simulations and actual protein motion. Preliminary results for Mb at 1666 cm^{-1} suggest that at least part of the conformational change occurs in 15 ps. These dynamics can be compared to indirect measurements which used resonance Raman spectroscopy to probe heme pocket relaxation.[20] These studies suggest that the tertiary structural changes in the position of the proximal histidine are complete within less than 30 ps. In these experiments, the Fe-N(his) stretching frequency reaches its equilibrium deoxy value within the 30 ps pulsewidth of the resonance Raman probe pulse. Another indirect measure of the protein response to CO photodissociation was obtained by Miller *et. al.* from picosecond phase grating spectroscopy.[28] These results suggest that a global change in the protein structure is occuring in less than 30 ps. In contrast, Simon *et. al.* report that relaxation of the transient circular dichroism spectrum probed at 355 nm of photodissociated MbCO to the equilibrium deoxy spectrum requires 300 ps.[15] The differences among all of these measurements may be due to the differences in what is being probed. In our TRIR measurements at 1666 cm^{-1} we are probing a specific part of the protein backbone structure. Measurements at other frequencies may reveal dynamics which correspond to the processes observed in other transient experiments.

In conclusion, we have demonstrated that TRIR in the amide I region gives structural information regarding protein conformational changes in real time. Assignment of many of the amide I peaks to specific amide or sidechain structures will require much additional effort. It is clear, however, that enormous potential exists for elucidating structural relaxation dynamics and energetics with a high degree of structural specificity using this approach. In addition, our work demonstrates that TRIR difference spectra avoid many of the difficulties associated with steady-state FTIR spectra; explicit subtraction of water and water vapor backgrounds is unnecessary, as are mathematical enhancement techniques. This is an advantage because enhancement of steady-state FTIR spectra is only likely to be useful for small, water-soluble proteins, where criteria for subtraction of water background have been developed. In addition, TRIR difference spectra are sensitive only to the active parts of the protein rather than all infrared absorbers, and are therefore more generally applicable.

5. ACKNOWLEDGMENTS

Support for this work by LANL Institutional Supporting Research Grant X15B and by National Institutes of Health Grant GM 48509 is acknowledged. TPC acknowledges support from the Director's Fellowship program at LANL. This work was performed at Los Alamos National Laboratory under the auspices of the U. S. Department of Energy.

6. REFERENCES

1. Perutz, M.F.; Kendrew, J. C.; Watson, H. C. *J. Mol. Biol.* **1965**, *13*, 669-678; Brooks, C. L.; Karplus, M.; Pettitt, B. M. *Adv. Chem. Phys.* **1988**, *71*, 111.

2. Dyer, R. B.; Einarsdóttir, Ó.; Killough, P. M.; López-Garriga, J. J.; Woodruff, W. H. *J. Am. Chem. Soc.* **1989**, *111*, 7657-7659.
3. Elliott, A.; Ambrose, E. J. *Nature* **1950**, *165*, 921-922.
4. Dong, A.; Huang, P.; Caughey, W. S. *Biochemistry* **1990**, *29*, 3303-3308.
5. Dousseau, F.; Pézolet, M. *Biochemistry* **1990**, *29*, 8771-8779.
6. Dong, A.; Huang, P.; Caughey, W. S. *Biochemistry* **1992**, *31*, 182-189.
7. Kaiden, K.; Matsui, T.; Tanaka, S. *Appl. Spectros.* **1987**, *41*, 180-184.
8. Susi, H.; Byler, D. M. *Meth. Enzymol.* **1986**, *130*, 291-311.
9. Kuriyan, J.; Wilz, S.; Karplus, M.; Petsko, G. A. *J. Mol. Biol.* **1986**, *192*, 133-154.
10. Takano, T. *J. Mol. Biol.* **1977**, *110*, 569-584.
11. Henry, E. R.; Sommer, J. H.; Hofrichter, J.; Eaton, W. A. *J. Molec. Biol.* **1983**, *166*, 443-451.
12. Gibson, Q. H.; Olson, J. S.; McKinnie, R. E.; Rohlfs, R. J. *J. Biol. Chem.* **1986**, *261*, 10228-10239.
13. Petrich, J. W.; Poyart, C.; Martin, J. L. *Biochemistry* **1988**, *27*, 4049-4060; Petrich, J. W.; Martin, J. L. *Chem. Phys.* **1989**, *131*, 31-47.
14. Kottalam, J.; Case, D. A. *J. Am. Chem. Soc.* **1988**, *110*, 7690-7697.
15. Xie, X.; Simon, J. D. *Biochemistry* **1991**, *30*, 3682-3692.
16. Dixon, A. J.; Glyn, P.; Healy, M. A.; Hodges, P. M.; Jenkins, T.; Poliakoff, M.; Turner, J. J. *Spectrochim. Acta* **1988**, *44A*, 1309-1314.
17. Jedju, T. M.; Rothberg, L.; Labrie, A. *Opt. Lett.* **1988**, *13*, 961-963.
18. Anfinrud, P. A.; Han, C.; Hochstrasser, R. M. *Proc. Natl. Acad. Sci. USA* **1989**, *86*, 8387-8391.
19. Gerwert, K.; Rodriguez-Gonzalez, R.; Siebert, F., in *Time-resolved infrared spectroscopy applied to photobiological systems*; Laubereau, A.; Stockburger, M., Eds.; Springer-Verlag: Berlin, 1985, pp 263-268.
20. Findsen, E. W.; Friedman, J. M.; Ondrias, M. R.; Simon, S. R. *Science* **1985**, *229*, 661-665.
21. Westrick, J. A.; Goodman, J. L.; Peters, K. S. *Biochemistry* **1987**, *26*, 8313-8318.
22. Westrick, J. A.; Peters, K. S.; Ropp, J. D.; Sligar, S. *Biochemistry* **1990**, *29*, 6741-6746.
23. Stoutland, P. O.; Dyer, R. B.; Woodruff, W. H. *Science* **1992**, *257*, 1913-1917.
24. Yen, R.; Shank, C. V.; Hirlimann, C. *Mater. Res. Soc. Symp Proc.* **1983**, *13*, 13-16; Ma, H. M.; Liu, Y. X.; Fei, Y.; Li, F. M. *J. Appl. Phys.* **1989**, *65*, 5031-5034.
25. Chance, M. R.; Courtney, S. H.; Chavez, M. D.; Ondrias, M. R.; Friedman, J. M. *Biochemistry* **1990**, *29*, 5537-5545.
26. Surewicz, W. K.; Mantsch, H. H. *Biochim. Biophys. Acta* **1988**, *952*, 115-130.
27. Lambright, D. G.; Balasubramanian, S.; Boxer, S. G. *J. Mol. Biol.* **1989**, *207*, 289-299.
28. Richard, L.; Genberg, L.; Deak, J.; Chiu, H.-L.; Miller, R. J. D. *Biochemistry* **1992**, *31*, 10703-10715.